

Supporting Information
for
Amphiphilic Cyclodextrin-based Nanocarriers for Magnetic
Delivery of a Morphogen in Microfluidic Environments

Alessandro Surpi,^{*a†} Roberto Zagami,^{b,c†} Marianna Barbalinardo,^a Nina Burduja,^{b,c} Giuseppe Nocito,^b Riccardo Di Corato,^{d,e} Maria Pia Casaletto,^f Francesco Valle,^a Angelo Nicosia,^g Placido Giuseppe Mineo,^g Valentin Alek Dediu^a and Antonino Mazzaglia^{*b}

^a National Research Council, Institute for Nanostructured Materials (CNR-ISMN) Via Pietro Gobetti 101, 40129 Bologna, Italy.

^b National Research Council, Institute for Nanostructured Materials (CNR-ISMN), URT of Messina at Dept. of Chemical, Biological, Pharmaceutical and Environmental Sciences (ChiBioFarAm), University of Messina, Viale F. Stagno d'Alcontres 31, 98166 Messina, Italy.

^c Dept. of Chemical, Biological, Pharmaceutical and Environmental Sciences (ChiBioFarAm), University of Messina, Viale F. Stagno d'Alcontres 31, 98166 Messina, Italy.

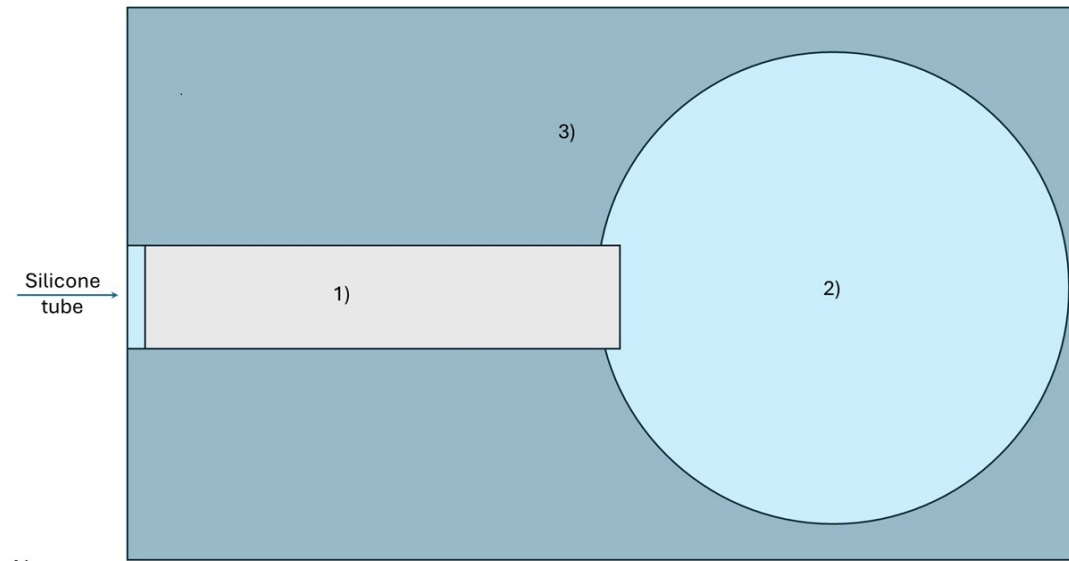
^d National Research Council, Institute for Microelectronics and Microsystems (CNR-IMM), SP Lecce-Monteroni Km 1,200, 73100 Lecce, Italy.

^e Center for Biomolecular Nanotechnologies, Istituto Italiano di Tecnologia, Arnesano 73010, Italy.

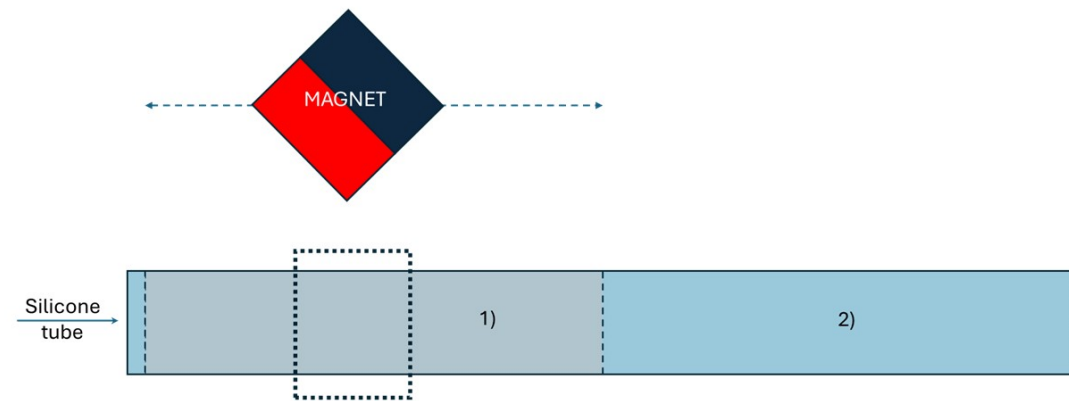
^f National Research Council, Institute for Nanostructured Materials (CNR-ISMN), Via Ugo La Malfa 153, 90146 Palermo, Italy.

^g Dept. of Chemical Sciences, University of Catania, Viale Andrea Doria 6, 95125 Catania, Italy.

† These authors contributed equally



A)



B)

Fig. S1 A) Plan view of the microfluidic chip: 1) quartz chip, 2) culture well, 3) PDMS slab in which the culture well is carved; B) Cross section of the microfluidic chip with informative sketch of magnets motions. Magnetic nanocarriers are concentrated into the dashed area between the magnets and, once there, solidly follow the magnets' motion along the capillary.

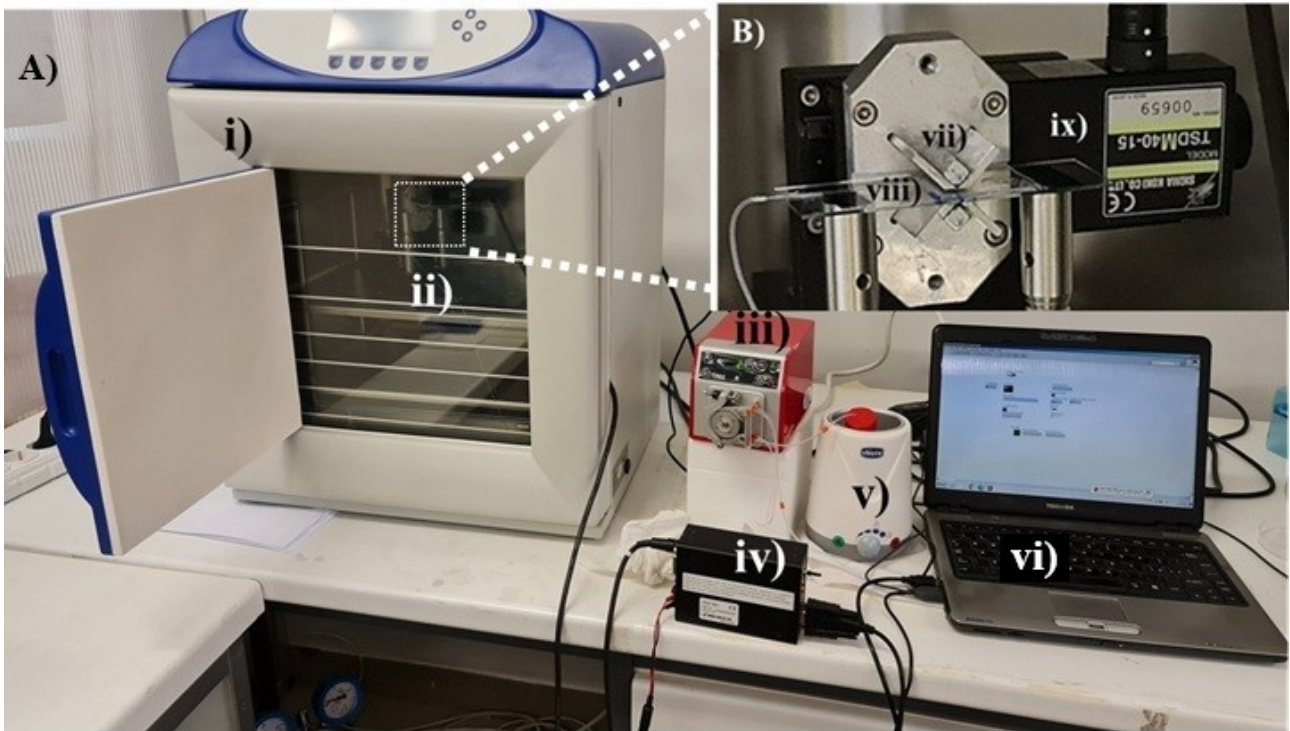


Fig. S2 Experimental set up configuration for magnetically controlled delivery of SPION/SC6OH/RA. A) Overview: i) incubator, ii) microfluidic chip and magnetic device (further enlarged in B), iii) peristaltic pump connected via silicone tube to the microfluidic chip, iv) motor controller, v) thermostatic bath, vi) computer. B) Zoom on (ii) microfluidic chip (Dashed area on A): vii) magnet (The other magnet is symmetrically placed under the microfluidic chip), viii) microfluidic chip, ix) linear motor.

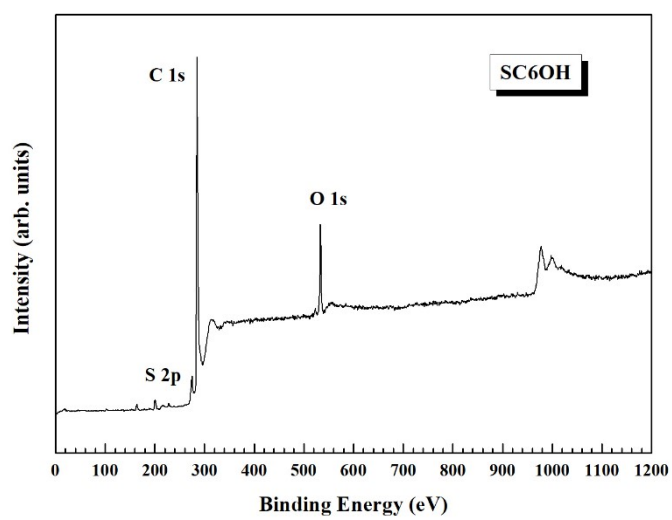
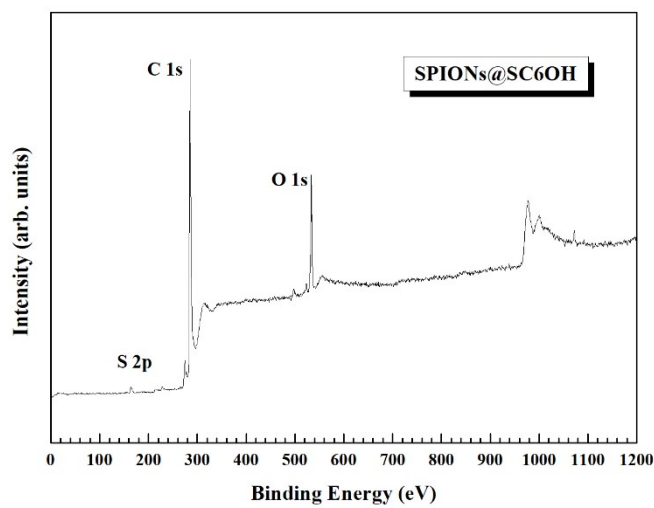
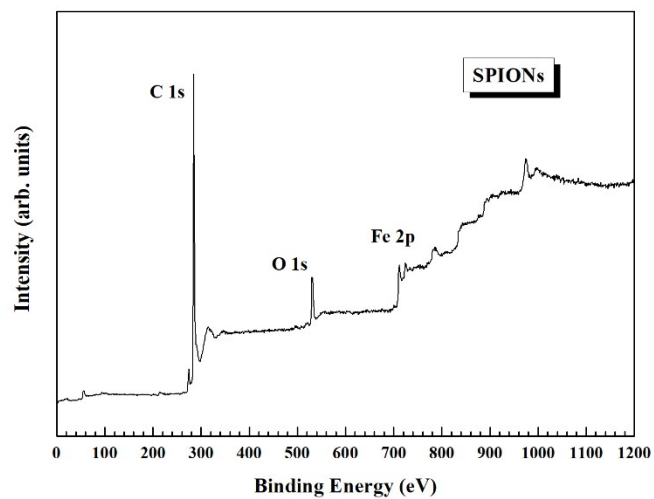


Fig. S3 XPS survey spectra of the investigated samples.

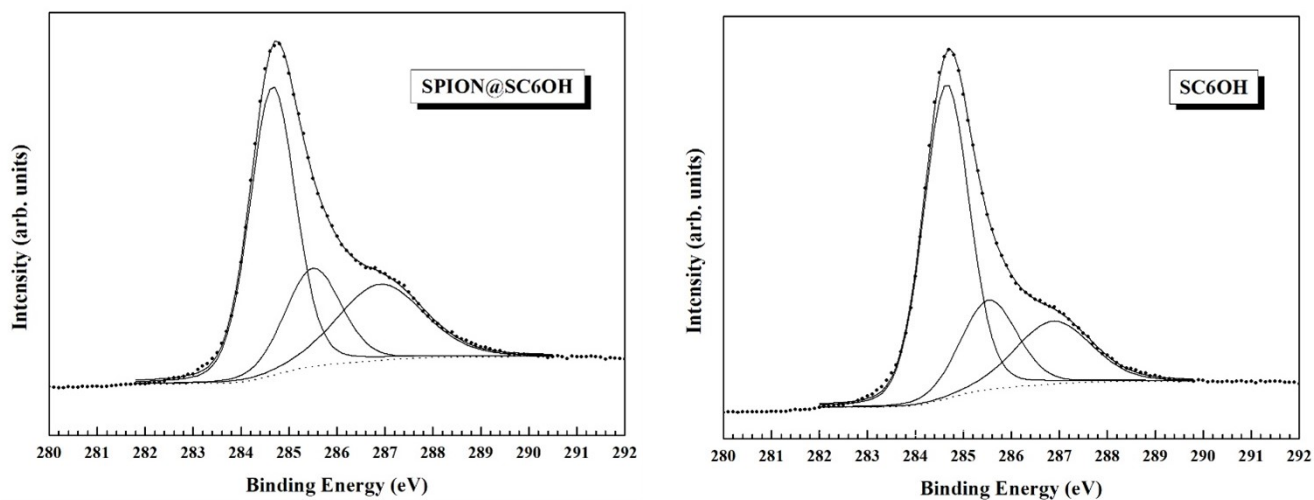


Fig. S4 XPS curve-fitting of C 1s spectra of the investigated samples.

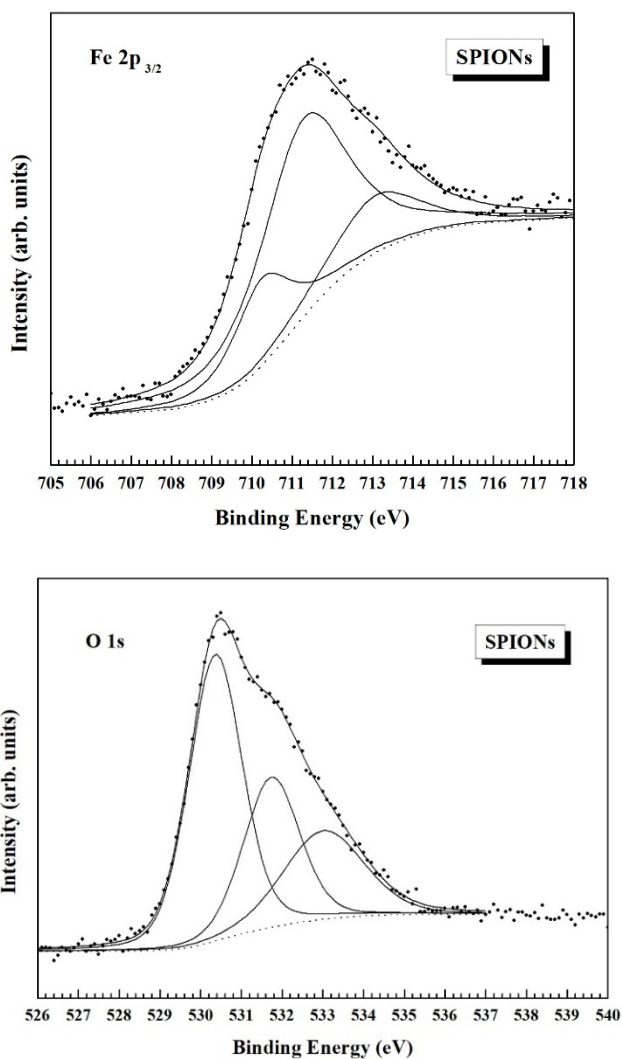


Fig. S5 Fe 2p_{3/2} and O 1s XPS curve-fitting in the SPION sample.

Table S1. Mean D_H , PDI and ζ -potential of SPION@SC6OH in ultrapure water

time / days	D_H / nm (Ampl. %)	PDI	ζ / mV
t = 0	260 ± 88 (89)	0.11	-34.1 ± 5.2
	20 ± 3 (11)	0.02	
t = 1	259 ± 114 (86)	0.19	-33.3 ± 5.0
	20 ± 4 (14)	0.04	
t = 3	254 ± 81 (82)	0.10	-33.4 ± 5.9
	22 ± 5 (18)	0.05	
t = 4	289 ± 71 (84)	0.06	-33.9 ± 5.7
	22 ± 4 (16)	0.03	
t = 7	376 ± 70 (85)	0.03	-34.2 ± 5.2
	27 ± 5 (15)	0.03	

(pH 5.5, T = 37 °C, SPION@SC6OH 0.17 mg/mL, [SC6OH] = 40 μ M).

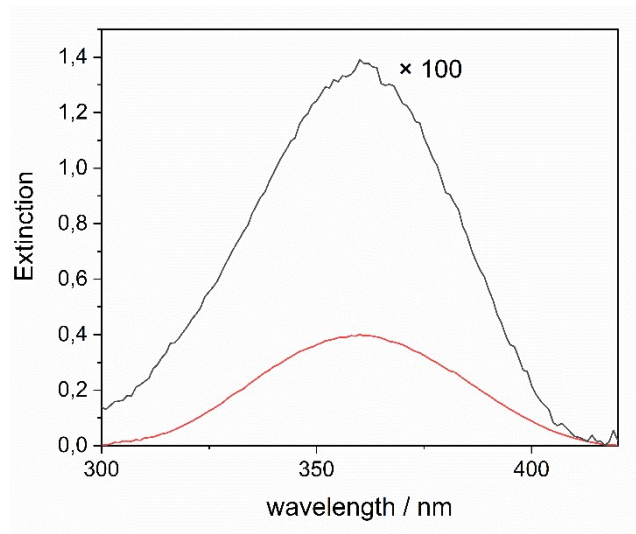


Fig. S6 UV/Vis spectra of the aqueous dispersions of SPION@SC6OH/RA (black line) and supernatant (red line) upon separation by applied magnetic field. Path length 0.1 cm. (UV/Vis spectrum of SPION@SC6OH/RA (black line) has been multiplied by a factor 100).

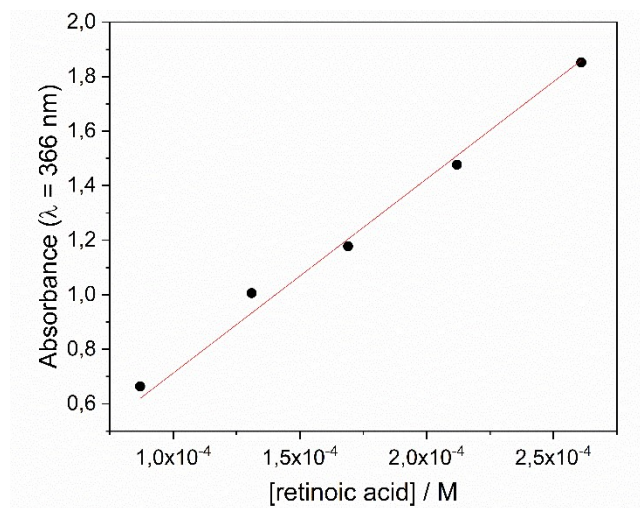


Fig. S7 Absorption calibration curve for retinoic acid in DCM. ($\epsilon_{366\text{nm}} = 3.3 \times 10^4 \text{M}^{-1} \cdot \text{cm}^{-1}$, $d = 0.2 \text{ cm}$ $R^2 = 0.989$).